

Advanced approach to design of small wind turbine support structures

Ismar Imamovic^{*1}, Suljo LJukovac^{1,2b} and Adnan Ibrahimbegovic^{2a}

¹University of Sarajevo-Faculty of Civil Engineering, Patriotske lige 30, Sarajevo, Bosnia and Herzegovina

²University of Technology Compiègne, Centre de Recherches Royallieu, Laboratory Roberval Mecanique,
60200 Compiègne, France

(Received May 23, 2022, Revised July 3, 2022, Accepted July 15, 2022)

Abstract. In this work we present an advanced approach to the design of small wind turbine support steel structures. To this end we use an improved version of previously developed geometrically exact beam models. Namely, three different geometrically exact beam models are used, the first two are the Reissner and the Kirchhoff beam models implementing bi-linear hardening response and the third is the Reissner beam capable of also representing connections response. All models were validated in our previous research for a static response, and in this work they are extended to dynamic response. With these advanced models, we can perform analysis of four practical solutions for the installation of small wind turbines in new or existing buildings including effects of elastoplastic response to vibration problems. The numerical simulations confirm the robustness of numerical models in analyzing vibration problems and the crucial effects of elastoplastic response in avoiding resonance phenomena.

Keywords: connection behavior; elastoplastic behavior; geometrically exact beam models; vibration problems; wind load

1. Introduction

The new concept of tall buildings with improved energy balance follows current world trends. In present time, when negative effects of global warming impact the world economy and lives of ordinary people, air pollution reduction and building energy balance improvement are imperative in urban areas. The large urban areas are the big consumers of energy for heating and cooling of living spaces. The world trend is the production of green energy, but still in many countries the most of their energy is obtained by burning the fossil fuels and emitting large amounts of greenhouse gases and air pollutants.

One of the ways in reducing global energy consumption is by improving the building energy balance in urban areas. The energy balance can be improved by using new structural materials, adding secondary elements for better heating and cooling, better disposition of building regarding

*Corresponding author, Assistant Professor, E-mail: imamovic.ismar@gmail.com

^aProfessor, E-mail: adnan.ibrahimbegovic@utc.fr

^bPh.D. Student, E-mail: Suljo.Ljukovac@gmail.com

usage of solar energy, etc. Active energy production is usually focused on large wind turbines, where improvement of efficiency by using flexible blades is the subject of research (Boujelben *et al.* 2020), which are not suitable for installation in an urban area. The second possibility for active energy production concerns the idea of using small wind turbines, which can be installed on roofs or facades of existing or new buildings.

In this work we explore the possibilities to add small wind turbines to existing or new buildings, and propose advanced numerical models able to deal with the dynamic response of supporting structures. The supporting structures for wind turbines are usually built of structural steel elements which have to connect to existing or new buildings. Namely, two different numerical models are required: the first capable of representing steel elements, and the second also including connection behavior in global response of secondary structure.

Steel as a construction material has good mechanical properties and ductile constitute behavior that allow producing thin elements subjected to instability issues (buckling) and large displacements. From a numerical point of view, the buckling phenomenon can be tackled by using the von Karman strain measure (Dujc *et al.* 2010, Hajdo *et al.* 2020) or by using the geometrically nonlinear models the Reissner beam (Ibrahimbegovic 1995, Imamovic *et al.* 2017) or the Kirchhoff beam (Imamovic *et al.* 2019). The ability to handle combination of large displacement and plastic behavior makes this element a robust tool for solving this type of problem. Finally, the commonly used assumption that wind load is a non-conservative and always perpendicular to the area, requires follower force definition (Hajdo *et al.* 2021).

The connections between wind turbine support steel structure and an existing or a new building can be built in many ways. Numerically, it can lowest be represented by a simple model of rotational springs according to modern Codes (EN 1993-1-8 2005) or in a better way by more advanced models. In this work, we use a previously developed geometrically exact beam models capable of representing complex connection response (Imamovic *et al.* 2018), which is further improved in this work by adding dynamic response.

With these models in hand, we analyze different solutions for small wind turbine installation to buildings, providing novel advanced approach for support structure design including vibration problem and flutter phenomena. The wind load is considered as dynamic load, and all proposed solution are designed according to modern code that provide real life numerical simulation.

The outline of the paper is as follows. In Section 2 are briefly recall the main equations of geometrically nonlinear models of Reissner beam and Kirchhoff beam, within dynamics framework. Section 3 deals with constitutive models for steel elements and structural connections, while Section 4 provides main information about numerical implementation. Three numerical simulations are presented in Section 5, dealing with the dynamic response of secondary steel structures for wind turbines and analyzing the effects of temperature change on dynamic response. In the last section, we state the conclusions.

2. Geometrically exact Reissner beam and Kirchhoff beam models

In this section we recall the main statement of theoretical formulation for two geometrically exact beam models, which are capable of representing large displacement elastoplastic material behavior and buckling phenomena. The theoretical formulation is defined by three equation sets: kinematics equations, constitutive equations, and equilibrium equations.

2.1 Geometrically nonlinear kinematics

In the framework of large displacement gradient theory, the position vector for Reissner's beam (Ibrahimbegovic and Frey 1993) in deformed configuration can be written as

$$\boldsymbol{\varphi} := \boldsymbol{\varphi}_0 + \zeta \mathbf{t} = \begin{pmatrix} x+u \\ y+v \end{pmatrix} + \zeta \begin{pmatrix} -\sin \psi \\ \cos \psi \end{pmatrix} \quad (1)$$

where x and y are coordinates in the reference configuration, u and v are displacement components in the global coordinate system, ζ is the coordinate along the normal to the beam axis in the reference configuration, and ψ is the section rotation. The corresponding form of the deformation gradient \mathbf{F} (see Ibrahimbegovic 2009) can be written as

$$\mathbf{F} := \nabla \boldsymbol{\varphi} = \underbrace{\begin{bmatrix} 1 + \frac{du}{dx} & 0 \\ \frac{dv}{dx} & 0 \end{bmatrix}}_{\mathbf{F}_{u,v} = \mathbf{I} + \nabla \mathbf{u}} + \underbrace{\begin{bmatrix} -\zeta \frac{d\psi}{dx} \cos \psi & -\sin \psi \\ -\zeta \frac{d\psi}{dx} \sin \psi & \cos \psi \end{bmatrix}}_{\mathbf{F}_\psi = \mathbf{I} + \nabla \psi} \quad (2)$$

By using the polar decomposition of the deformation gradient \mathbf{F} , we can obtain the multiplicative split into rotation \mathbf{R} and stretch \mathbf{U} , and thus define the corresponding rotated strain measure \mathbf{H}

$$\mathbf{F} = \mathbf{R}\mathbf{U} \rightarrow \mathbf{U} = \mathbf{R}^T \mathbf{F}, \quad \mathbf{R} = \begin{bmatrix} \cos \psi & -\sin \psi \\ \sin \psi & \cos \psi \end{bmatrix} \rightarrow \mathbf{H} = \mathbf{U} - \mathbf{I} \quad (3)$$

Furthermore, the stretch \mathbf{U} can be additively decomposed into stretch $\mathbf{U}_{u,v}$ related to displacement and stretch \mathbf{U}_ψ related to rotation

$$\mathbf{U} = \mathbf{U}_{u,v} + \mathbf{U}_\psi \quad (3)$$

where

$$\mathbf{U}_{u,v} = \begin{bmatrix} \left(1 + \frac{du}{dx}\right) \cos \psi + \frac{dv}{dx} \sin \psi & 0 \\ -\left(1 + \frac{du}{dx}\right) \sin \psi + \frac{dv}{dx} \cos \psi & 0 \end{bmatrix}; \quad \mathbf{U}_\psi = \begin{bmatrix} -\zeta \frac{d\psi}{dx} & 0 \\ 0 & 1 \end{bmatrix}; \quad \mathbf{I} = \begin{bmatrix} 1 & 0 \\ 0 & 1 \end{bmatrix}$$

The rotated strain measure components proposed by Reissner (1972) can be written as

$$\begin{aligned} \Sigma &= H_{11} - \zeta K = \left(1 + \frac{du}{dx}\right) \cos \psi + \frac{dv}{dx} \sin \psi - 1 \\ \Gamma &= H_{21} = -\left(1 + \frac{du}{dx}\right) \sin \psi + \frac{dv}{dx} \cos \psi \\ K &= \frac{d\psi}{dx} \end{aligned} \quad (4)$$

where Σ and Γ are, respectively, the axial and shear strain in rotated configuration and K is the curvature strain.

The results in Eqs. (4)₁ and (4)₂ can be rewritten in compact matrix notation as

$$\begin{aligned} \Sigma &= (\Sigma, \Gamma)^T = \Lambda^T (\mathbf{h}(\mathbf{a}) - \Lambda) \\ \Lambda &= \begin{bmatrix} \cos \psi & -\sin \psi \\ \sin \psi & \cos \psi \end{bmatrix}; \mathbf{h}(\mathbf{a}) = \begin{pmatrix} 1 + \frac{du}{dx} \\ \frac{dv}{dx} \end{pmatrix} \end{aligned} \quad (5)$$

By imposing at this stage Kirchhoff's constraint, implying that the beam section remains not only plane but also perpendicular to the beam axis resulting in zero shear strain ($\Gamma = 0$). Thus we further obtain

$$\tan \psi = \frac{\frac{dv}{dx}}{1 + \frac{du}{dx}} \Rightarrow \tilde{\psi} = \arctan \left(\frac{\frac{dv}{dx}}{1 + \frac{du}{dx}} \right) \quad (6)$$

With vanished shear deformation, the Eq. (5) can be rewritten as

$$\Sigma = (\Sigma, \Gamma = 0)^T = \tilde{\Lambda}^T (\mathbf{h}(\mathbf{a}) - \tilde{\Lambda}); \tilde{\Lambda} = \begin{bmatrix} \cos \tilde{\psi} & -\sin \tilde{\psi} \\ \sin \tilde{\psi} & \cos \tilde{\psi} \end{bmatrix} \quad (7)$$

By exploiting the result in (6) and in (4)₃ we can obtain the corresponding expression for the curvature of the geometrically exact Kirchhoff beam

$$\begin{aligned} K &= \frac{d\tilde{\psi}}{dx} = \frac{-\left(\frac{d^2u}{dx^2}\right)\left(\frac{dv}{dx}\right) + \left(\frac{d^2v}{dx^2}\right)\left(1 + \frac{du}{dx}\right)}{\left(1 + \frac{du}{dx}\right)^2 + \left(\frac{dv}{dx}\right)^2} = \left(\frac{d^2v}{dx^2} \cos \tilde{\psi} - \frac{d^2u}{dx^2} \sin \tilde{\psi}\right) \frac{1}{\Delta l} = \\ &= \frac{d\tilde{\Lambda}^T}{d\tilde{\psi}} \frac{d\mathbf{h}(\mathbf{a})}{dx} \frac{1}{\Delta l} \end{aligned} \quad (8)$$

where

$$\frac{d\tilde{\Lambda}^T}{d\tilde{\psi}} = (-\sin \tilde{\psi} \quad \cos \tilde{\psi})^T; \frac{d\mathbf{h}(\mathbf{a})}{dx} = \begin{pmatrix} \frac{d^2u}{dx^2} \\ \frac{d^2v}{dx^2} \end{pmatrix}; \Delta l = \sqrt{\left(1 + \frac{du}{dx}\right)^2 + \left(\frac{dv}{dx}\right)^2}$$

2.2 Constitutive equations

It is well known that steel elements and structural connections behavior cannot be represented by the same constitutive relations. In this section we briefly recall two different constitutive

models. The first is capable of representing the behavior of steel elements, and the second a structural connection behavior.

The constitutive equations for finite strain beam in terms of Biot's stress resultants and rotated strain measure are chosen. The first step is the additive decomposition of the displacement and rotation gradients into elastic part (\bullet^e) and plastic part (\bullet^p), which corresponds to the multiplicative decomposition of the deformation gradient

$$\begin{aligned} \mathbf{F} &= \mathbf{I} + \nabla \mathbf{u}^e + \nabla \mathbf{u}^p + \mathbf{I} + \nabla \tilde{\psi}^e + \nabla \tilde{\psi}^p = \\ &= (\mathbf{I} + \nabla \mathbf{u}^e) (\mathbf{I} + \nabla \mathbf{u}^p (\mathbf{I} + \nabla \mathbf{u}^e)^{-1}) + (\mathbf{I} + \nabla \tilde{\psi}^e) (\mathbf{I} + \nabla \tilde{\psi}^p (\mathbf{I} + \nabla \tilde{\psi}^e)^{-1}) = \mathbf{F}_{u,v}^e \mathbf{F}_{u,v}^p + \mathbf{F}_{\psi}^e \mathbf{F}_{\psi}^p \end{aligned} \quad (9)$$

We also note that such multiplicative decomposition of the deformation gradient leads to the additive decomposition of the stretch tensor \mathbf{U} (Imamovic *et al.* 2017)

$$\mathbf{U} = \mathbf{R}^T (\mathbf{I} + \nabla \mathbf{u}^e + \nabla \mathbf{u}^p) + \mathbf{R}^T (\mathbf{I} + \nabla \tilde{\psi}^e + \nabla \tilde{\psi}^p) = \underbrace{\mathbf{U}_{u,v}^e + \mathbf{U}_{u,v}^p}_{\mathbf{U}_{u,v}} + \underbrace{\mathbf{U}_{\psi}^e + \mathbf{U}_{\psi}^p}_{\mathbf{U}_{\psi}} \quad (10)$$

where

$$\begin{aligned} \mathbf{U}_{u,v}^e &= \begin{bmatrix} \left(1 + \frac{du^e}{dx}\right) \cos \tilde{\psi} + \frac{dv}{dx} \sin \tilde{\psi} & 0 \\ -\left(1 + \frac{du^e}{dx}\right) \sin \tilde{\psi} + \frac{dv}{dx} \cos \tilde{\psi} & 0 \end{bmatrix}; \mathbf{U}_{\psi}^e = \begin{bmatrix} -\zeta \frac{d\tilde{\psi}^e}{dx} & 0 \\ 0 & 1 \end{bmatrix} \\ \mathbf{U}_{u,v}^p &= \begin{bmatrix} \frac{du^p}{dx} \cos \tilde{\psi} + \frac{dv^p}{dx} \sin \tilde{\psi} & 0 \\ -\frac{du^p}{dx} \sin \tilde{\psi} + \frac{dv^p}{dx} \cos \tilde{\psi} & 0 \end{bmatrix}; \mathbf{U}_{\psi}^p = \begin{bmatrix} -\zeta \frac{d\tilde{\psi}^p}{dx} & 0 \\ 0 & 0 \end{bmatrix} \end{aligned}$$

The Helmholtz free energy can be defined as a quadratic form

$$\Psi(\mathbf{U}^e, \boldsymbol{\xi}^p) = \underbrace{\frac{1}{2} \mathbf{U}^{e,T} \cdot \mathbf{C}^e \cdot \mathbf{U}^e}_{\Psi^e} + \underbrace{\frac{1}{2} \boldsymbol{\xi}^{p,T} \cdot \mathbf{K}^h \cdot \boldsymbol{\xi}^p}_{\Xi^p} \quad (11)$$

where \mathbf{U}^e is the elastic part of the stretch tensor, $\boldsymbol{\xi}^p$ is the vector of hardening variables, and \mathbf{K}^h are the corresponding hardening moduli. The yield criterion condition is composed of three or two multisurface plasticity criteria, depending on vanishing shear deformation or not. The first is related to the axial force, the second to the bending moment, and the third to the shear force. All criteria are postulated in terms of stress resultants of the Biot stress, imposing that

$$\bar{\phi}(\mathbf{T}, \bar{\mathbf{q}}) \leq \mathbf{T} - (\mathbf{T}_y - \mathbf{q}) \quad (12)$$

where: $\mathbf{q} = [q^N, q^M, q^S]$ is the vector of internal hardening stress like variables related to the axial force, bending moment, and shear force, respectively; and $\mathbf{T}_y = [N_y, M_y, S_y]$ are the yield stress resultants of Biot stress, axial force, bending moment, and shear force. The interaction between axial force and bending moment is included according to modern design code (EN 1993-1-8 2005), concerned with the reduction of yield bending moments depending on axial force intensity. The reduction for I section profile is

$$\begin{aligned}
 & \text{IF } \begin{matrix} N \leq 0.25N_y \\ N \leq 0.5A_w f_y \end{matrix} \text{ then no reduction } M_y^N = M_y \\
 & \text{ELSE } M_y^N = M_y \left[1 - \left(\frac{n-a}{1-a} \right) \right]; \quad n = \frac{N}{N_y}; \quad a = \frac{A_w}{A} \leq 0.5
 \end{aligned} \tag{13}$$

where A_w is web area and f_y is yield stress.

The second principle of thermodynamics (Ibrahimbegovic 2009) can be used to state that the plastic dissipation must remain non-negative

$$0 \leq \mathcal{D} = \underbrace{\left(\mathbf{T} - \frac{d\Psi^e}{d\mathbf{U}^e} \right) \dot{\mathbf{U}}^e}_{\mathcal{D}^e=0} + \underbrace{\mathbf{T} \dot{\mathbf{U}}^p - \frac{\partial \Xi^p}{\partial \boldsymbol{\xi}^p} \frac{d\boldsymbol{\xi}^p}{dt}}_{\mathcal{D}^p} \tag{14}$$

The principle of maximum plastic dissipation (Hill 1950) can then be enforced to obtain the corresponding evolution equations of plastic strain and hardening variable. This principle can be formulated as the constrained minimization problem, where the constraint is the yield function in (12). For more details see (Imamovic *et al.* 2017, 2019, Ibrahimbegovic 2009).

The constitutive model capable of representing structural connection behavior, previously developed by authors, was inspired by experimental test results, see (Imamovic *et al.* 2018). Namely, the large deformations of structural connection under cyclic loading cause a less stiff response in opposite direction. This phenomenon has a physical explanation. During the loading of the experimental structure, large deformations of the welded plate in the tension zone cause a partial loss of the contact between the plate and horizontal beam, see Fig. 1(a). With the change in the direction of the applied load, the compression and tension zones will be inverted. The partially lost contact in the compression zone causes the reduced stiffness of the connection, see Fig. 1(b). The stiffness remains reduced until the full contact between the plate and horizontal beam is reached again. After the full contact has been reached, the connection will provide again the full stiffness.

This phenomenon can be captured with contact and solid elements in refined FEM models. However, the refined FEM models are too complex for everyday usage. For this reason, we propose the use of the beam element capable of representing the mentioned phenomenon.

The idea is to use the coupled plasticity-damage model (Imamovic *et al.* 2015). The plasticity part governs the hardening and unloading phases, whereas the damage part provides the reduced



Fig. 1 Deformation of the connection during a cyclic loading

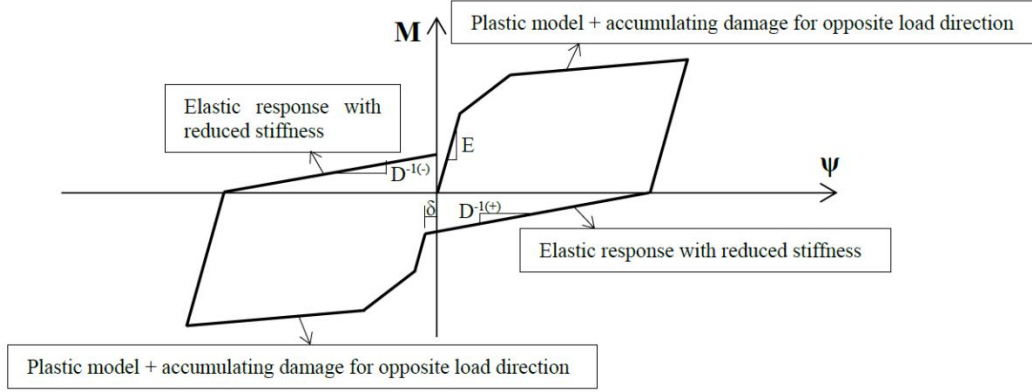


Fig. 2 Constitutive model

stiffness of the connection after the change in the sign of the bending moment: from positive to negative or vice versa, see Fig. 2. The damage model governs connection response until full contact between the plate and horizontal beam is reached. After the full contact has been reached, the plasticity model is again activated. The gap δ corresponds to the plastic deformation in bolts.

The constitutive model of the beam consists of bilinear hardening and linear softening (Imamovic *et al.* 2017). The hardening model is defined as coupled plasticity-damage model. The modification of the beam model requires the splitting of internal variables into two groups, depending on the sign of the bending moment. This model is capable of representing a previously described phenomenon that is commonly observed during experimental testing. A brief description of the beam's constitutive model is given as follows.

The Helmholtz free energy can be defined in a quadratic form, for both, a positive ($\bar{\Psi}^{(+)}$) and a negative ($\bar{\Psi}^{(-)}$) value of the bending moment (M)

$$\begin{aligned}
 \Psi^{(+)}(\mathbf{U}^{e,(+)}, \xi^{p,(+)}, \mathbf{U}^{d,(+)}, \xi^{d,(+)}) &= \underbrace{\frac{1}{2} \mathbf{U}^{e,T,(+)} \cdot \mathbf{C}^{(+)} \cdot \mathbf{U}^{e,(+)}}_{\bar{\Psi}^{e,(+)}} + \underbrace{\frac{1}{2} \xi_1^{p,T,(+)} \cdot \mathbf{K}_1^{h,(+)} \cdot \xi_1^{p,(+)}}_{\bar{\Xi}_1^{p,(+)}} + \\
 &+ \underbrace{\frac{1}{2} \xi_2^{p,T,(+)} \cdot \mathbf{K}_2^{h,(+)} \cdot \xi_2^{p,(+)}}_{\bar{\Xi}_2^{p,(+)}} + \underbrace{\mathbf{T} \mathbf{U}^{d,(+)} - \frac{1}{2} \mathbf{T} \mathbf{D}^{(+)} \mathbf{T}}_{\bar{\Psi}^{d,(+)}} + \underbrace{\frac{1}{2} \xi_5^{d,(+)} \mathbf{K}^{d,(+)} \xi_5^{d,(+)}}_{\bar{\Xi}_5^{d,(+)}} \\
 \Psi^{(-)}(\mathbf{U}^{e,(-)}, \xi^{p,(-)}, \mathbf{U}^{d,(-)}, \xi^{d,(-)}) &= \underbrace{\frac{1}{2} \mathbf{U}^{e,T,(-)} \cdot \mathbf{C}^{(-)} \cdot \mathbf{U}^{e,(-)}}_{\bar{\Psi}^{e,(-)}} + \underbrace{\frac{1}{2} \xi_1^{p,T,(-)} \cdot \mathbf{K}_1^{h,(-)} \cdot \xi_1^{p,(-)}}_{\bar{\Xi}_1^{p,(-)}} + \\
 &+ \underbrace{\frac{1}{2} \xi_2^{p,T,(-)} \cdot \mathbf{K}_2^{h,(-)} \cdot \xi_2^{p,(-)}}_{\bar{\Xi}_2^{p,(-)}} + \underbrace{\mathbf{T} \mathbf{U}^{d,(-)} - \frac{1}{2} \mathbf{T} \mathbf{D}^{(-)} \mathbf{T}}_{\bar{\Psi}^{d,(-)}} + \underbrace{\frac{1}{2} \xi_5^{d,(-)} \mathbf{K}^{d,(-)} \xi_5^{d,(-)}}_{\bar{\Xi}_5^{d,(-)}}
 \end{aligned} \tag{15}$$

where: $\mathbf{U}^e, \mathbf{U}^d$ are elastic and damage strain measure tensors; ξ_i^p, ξ_i^d are vectors of hardening variables of the plastic and damage model, respectively; D is the internal damage variable; $\mathbf{K}_i^h, \mathbf{K}^d$ are the corresponding hardening moduli of the plastic and damage model; and \mathbf{T} is Biot's stress tensor. Every symbol contains two symbols. The first corresponds to the positive ($\bullet^{(+)}$), and the second to the negative ($\bullet^{(-)}$) bending moment. The yield criterion, defined as multi-criteria

(plasticity and damage), can be completely different for the positive and the negative bending moment. However, in this work we have assumed that the response in the hardening regime is symmetric and defined by

$$\begin{aligned} \phi_i^p(T_i, q_i^p) &\leq 0 \\ \phi_i^d(T_i, q_i^d) &\leq 0 \end{aligned} \tag{16}$$

where \mathbf{q} is the vector of internal hardening stress-like variables. The second principle of thermodynamics states that the plastic dissipation must remain non-negative

$$\begin{aligned} 0 \leq \mathcal{D} = & \underbrace{\dot{\mathbf{T}} \left(\frac{\partial \chi^e}{\partial \mathbf{T}} - \mathbf{U}^e \right)}_{\mathcal{D}^e=0} + \underbrace{\dot{\mathbf{T}} \left(\frac{\partial \chi^d}{\partial \mathbf{T}} - \mathbf{U}^d \right)}_{\mathcal{D}^p} + \underbrace{\mathbf{T} \dot{\mathbf{U}}_1 - \frac{\partial \Xi_1^p}{\partial \xi_1^p} \frac{d\xi_1^p}{dt}}_{\mathcal{D}_1^p} + \\ & + \underbrace{\mathbf{T} \dot{\mathbf{U}}_2 - \frac{\partial \Xi_2^p}{\partial \xi_2^p} \frac{d\xi_2^p}{dt}}_{\mathcal{D}_2^p} + \underbrace{\frac{\partial \mathbf{U}^d}{\partial D} \dot{D} - \frac{\partial \Xi^d}{\partial \xi^d} \dot{\xi}^d}_{\mathcal{D}^d} \end{aligned} \tag{17}$$

where χ is complementary energy, see (Ibrahimbegovic 2009). The principle of maximum plastic dissipation can be formulated (Hill 1950, Ibrahimbegovic and Frey 1993) as the minimization problem with the constraint, with the latter being yield function (16).

2.3 Equilibrium equations

The weak form of the equations of motion is provided by the d’Alembert principle, which postulates that the snap-shot of motion taken at time ‘ t ’ can be described formally with the dynamic equilibrium equations. Unlike the statics problem, these equilibrium equations should also include the work of inertia forces, which are proportional to mass and directed opposite to acceleration. In such an approach, the fixed time ‘ t ’ corresponds to a particular deformed configuration, and hence virtual displacement field is considered to be independent of time. The weak form of equilibrium of equation in the material description, see (Ibrahimbegovic 2009), can be written as

$$G(\mathbf{a}, \hat{\mathbf{a}}) := \int_L \delta \mathbf{u}^T \mathbf{f}_i dx + \int_L \delta \Sigma N dx + \int_L \delta \Gamma S dx + \int_L \delta K M dx - G^{ext} = 0 \tag{18}$$

where $\delta \mathbf{u}^T = (\delta u \ \delta v \ \delta \theta)$ is a vector of virtual displacement components, and rotations; $\delta \Sigma, \delta \Gamma, \delta K$ are virtual components of rotated strain measure (see Imamovic *et al.* 2017, 2019); N, S, M are stress resultant forces, axial force, shear force, and bending moment, respectively; f_i is the inertial force vector, which can be determined from the kinetic energy by using the Lagrange’s equation of motion

$$\mathbf{f}_i = \frac{d}{dt} \left(\frac{\partial \mathbf{E}_k}{\partial \dot{\mathbf{u}}} \right) - \left(\frac{\partial \mathbf{E}_k}{\partial \mathbf{u}} \right) \tag{19}$$

The kinetic energy E_k is expressed in terms of mass density ρ and velocity components in deformed configuration, which can be derived from position vector φ related to reference coordinates

$$\dot{\boldsymbol{\phi}} = \frac{d}{dt} \boldsymbol{\phi} = \frac{d}{dt} \left(\begin{pmatrix} x+u \\ v \end{pmatrix} + \zeta \begin{pmatrix} -\sin\psi \\ \cos\psi \end{pmatrix} \right) = \begin{pmatrix} \dot{u} \\ \dot{v} \end{pmatrix} + \zeta \begin{pmatrix} -\dot{\psi} \cos\psi \\ -\dot{\psi} \sin\psi \end{pmatrix} \quad (20)$$

where ζ is the coordinate along the normal to the beam axis in the reference configuration. With these results in hand, we can express kinetic energy

$$E_k = \frac{1}{2} \rho \int_L \int_A \dot{\boldsymbol{\phi}}^T \dot{\boldsymbol{\phi}} dA dx = \frac{1}{2} \dot{\mathbf{u}}^T \mathbf{M} \dot{\mathbf{u}} \quad (21)$$

where $\dot{\mathbf{u}}^T = (\dot{u} \quad \dot{v} \quad \dot{\theta})$ is velocity vector components along the coordinate axes and rotational velocity, and \mathbf{M} is a constant mass matrix

$$\mathbf{M} = \begin{bmatrix} m_{u,v} & 0 & 0 \\ 0 & m_{u,v} & 0 \\ 0 & 0 & m_\psi \end{bmatrix}; \quad m_{u,v} = \int_A \rho dA \quad (22)$$

$$m_\psi = \int_A \rho \zeta^2 dA$$

By using previously defined kinetic energy, inertial forces can be expressed as

$$\mathbf{f}_i = \frac{d}{dt} \left(\frac{\partial E_k}{\partial \dot{\mathbf{u}}} \right) - \left(\frac{\partial E_k}{\partial \mathbf{u}} \right) = \frac{d}{dt} (\mathbf{M} \dot{\mathbf{u}}) - 0 = \mathbf{M} \ddot{\mathbf{u}} \quad (23)$$

The final step needed for numerical implementation is the linearization of the weak form of equilibrium equations so that an iterative strategy can be employed. It can be obtained by the consistent linearization of the expression (18) to get

$$\begin{aligned} L(G)|_{\mathbf{a}} &= G(\delta \mathbf{a}, \mathbf{a})|_{\mathbf{a}} + \frac{d}{d\beta} \left[G(\delta \mathbf{a}, \mathbf{a} + \beta \Delta \mathbf{a}) \right] \Big|_{\beta} = \\ &= G(\delta \mathbf{a}, \mathbf{a}) + \int_L \left(\mathbf{d}(\delta \mathbf{a}) \quad \frac{d\mathbf{d}(\delta \mathbf{a})}{dx} \right) \left[\mathbf{D}^T + \mathbf{D}^K \right] \begin{pmatrix} \mathbf{d}(\Delta \mathbf{a}) \\ \frac{d\mathbf{d}(\Delta \mathbf{a})}{dx} \end{pmatrix} dx; \end{aligned} \quad (24)$$

where \mathbf{D}^T and \mathbf{D}^K are tangent stiffness related to axial and bending response, while the inertia forces are included in $G(\mathbf{a}, \delta \mathbf{a})$.

3. Numerical simulations

In this section, we present the results of four numerical simulations of practical interest in the design of small wind turbine support structures. The different cases of installation on a new or existing building are analyzed. Those numerical simulations have been performed by using here described beam models, which were implemented in open-source software FEAP (University of California, Berkeley).

The first example deals with a small wind turbine added to the roof of a building, where we analyze a fixed column as the support structure under extreme conditions. In the second example, the wind turbine support structure in case of installation between two buildings is a focus of analysis. The support structure is one beam with a fixed end on one side, while the second side is also fixed but released for axial deformation regarding a temperature variation. The next example

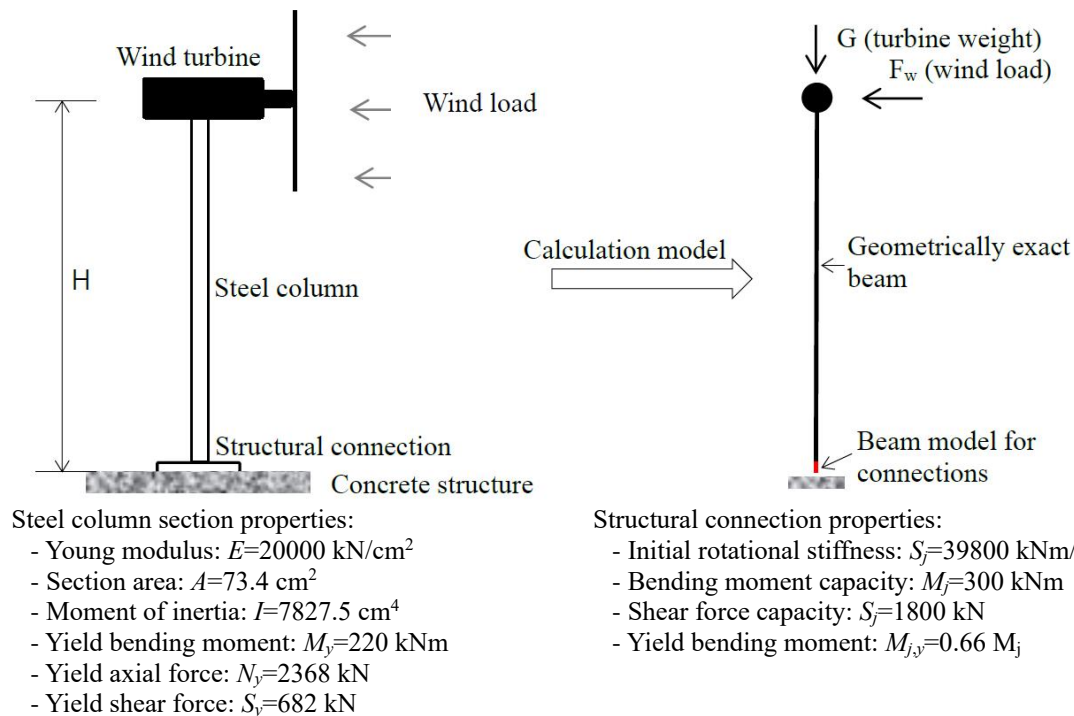


Fig. 3 Wind turbine structure vs. calculation model

is similar to the second but includes the effects of the temperature variations on the support structure response under extreme conditions. In the last simulation, we propose an innovative joint between elements of the support structure, which dissipates energy and has a function of frictional damping (Ibrahimbegovic and Mejia Nava 2021).

In order to show real-life cases, we have chosen 15-20 kW wind turbines in all numerical examples. Those wind turbines have a blade span of 6-10 m, so for the region of Sarajevo, Bosnia and Herzegovina, we obtain a design wind force of 20 kN, while the estimated weight of the wind turbine is 500 kg.

3.1 Wind turbine installation to the roof of a building

In this example, the simplest case of wind turbine support structure is analyzed, which can be installed on the roof of buildings, either existing or new. The support structure is one 6 m height steel column fixed to the roof of a building, while at the top is placed the wind turbine, see Fig. 3. The dimension of the steel column has been designed according to modern codes, so that the required cross-section is a round tube with a diameter of 300 mm and a wall thickness of 8 mm. This column is fixed to a concrete structure by base plate connection type, which is designed according to modern codes in a way that has a load-bearing capacity 35% bigger than the column has. According to Eurocode 3 (2005) at 66% of load-bearing capacity, the plastic deformation in connection elements begins and can be crucial to the dynamic response of the wind turbine support structure.

On the other side, the wind load value is determined according to modern codes also, which

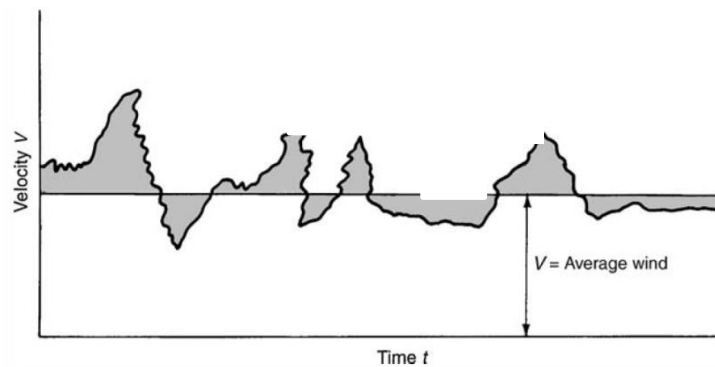


Fig. 4 Typical wind speed diagram

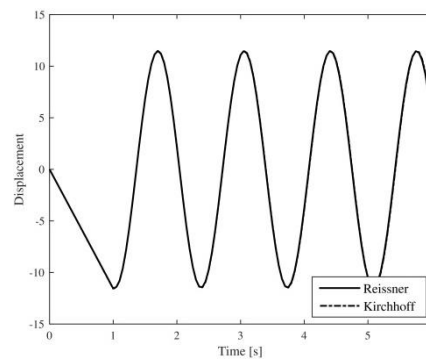


Fig. 5 Free vibrations

provides characteristic static load including all dynamic phenomenon. In this work, we decompose wind load into static and dynamic components, see Fig. 4. The static part corresponds to the average value of wind speed (corresponding force is equal to 20 kN), while the second dynamic part, we represent by a harmonic sine function with a value equal to 20% of design load. In order to test the dynamic response of the structure, the frequency of the harmonic load part is changed from 1.2 Hz to 0.2 Hz.

It is known that the dynamic response of a structure depends on how close are the eigenvalue frequency and load frequency because of that modern codes for wind loads provide procedures to avoid resonance phenomenon.

To obtain the eigenvalue frequency of the structure, we have first performed the analysis of free vibration with two beam model types, the Reissner beam, and the Kirchhoff beam. The dynamic analysis results of the structure for the free vibration problem are shown in Fig. 5, where we can see that both beam models provide the same results and the first eigenvalue period is equal to 1.35s ($f=1/1.35=0.74$ Hz).

The dynamic analyses for wind load (Fig. 4) are performed for three different load frequencies (0,2 Hz, 0,7 Hz, and 1.2 Hz) with three different beam models, where the last includes connection behavior. The results are shown in Figs. 6 and 7.

By analyzing Fig. 6, we can conclude that connection reduces vibration amplitude a little if the load frequency is sufficiently different from the eigenvalue frequency and connection behavior is

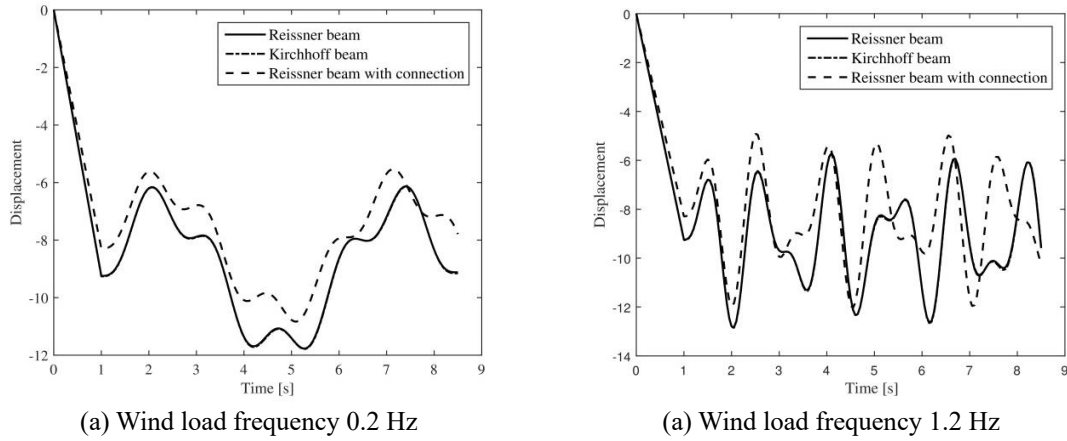


Fig. 6 Response of wind turbine structure-vibration amplitude

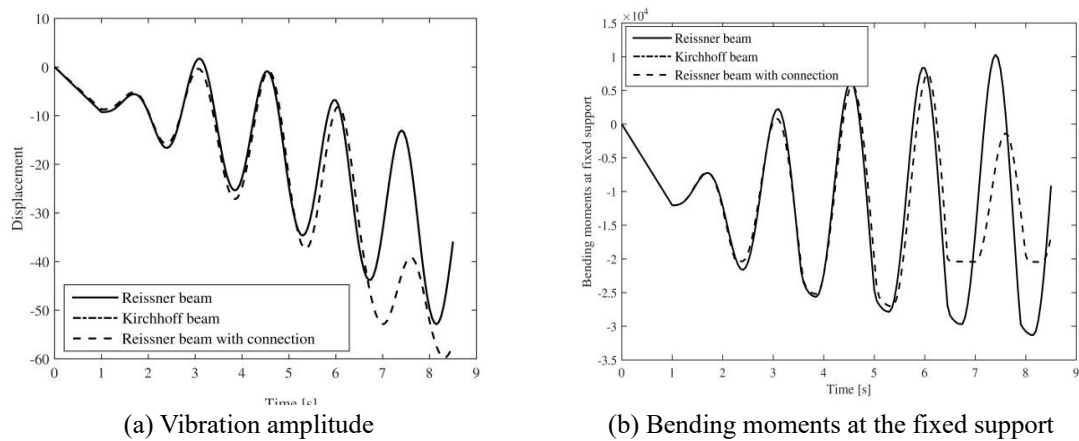


Fig. 7 Response of wind turbine structure under dynamic load with frequency 0.7 Hz

not so important for vibration amplitude. On the other side, if load frequency is close to eigenvalue frequency, the connection behavior can be crucial in avoiding resonance phenomena. Namely, structural connections usually reach the plastic threshold earlier than the rest of a structure. For example, in endplate connection and also base plate connection, plastic deformation starts at approximately 66% of bending capacity. These plastic deformations in connections play a very important role in damping vibration amplitude, see Fig. 7(b). Thus, it is very important to get the reliable estimates.

3.2 Wind turbine installed between two parts of a building

In this example, we analyze the second solution for small wind turbine installation on existing or new buildings. The small wind turbine can be installed at the secondary steel beam added between two buildings or two parts of one building, see Fig. 8. This computation is performed by using Reissner and Kirchhoff beam models for representing steel elements response, while the fixed connections at both ends are included with the previously described beam model for

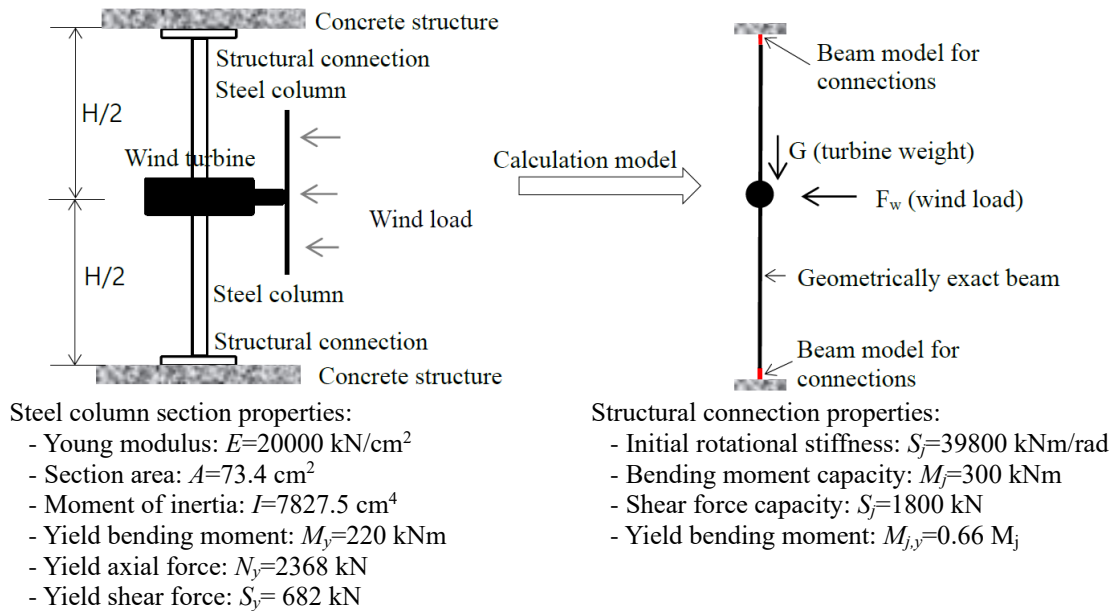


Fig. 8 Wind turbine structure vs. calculation model

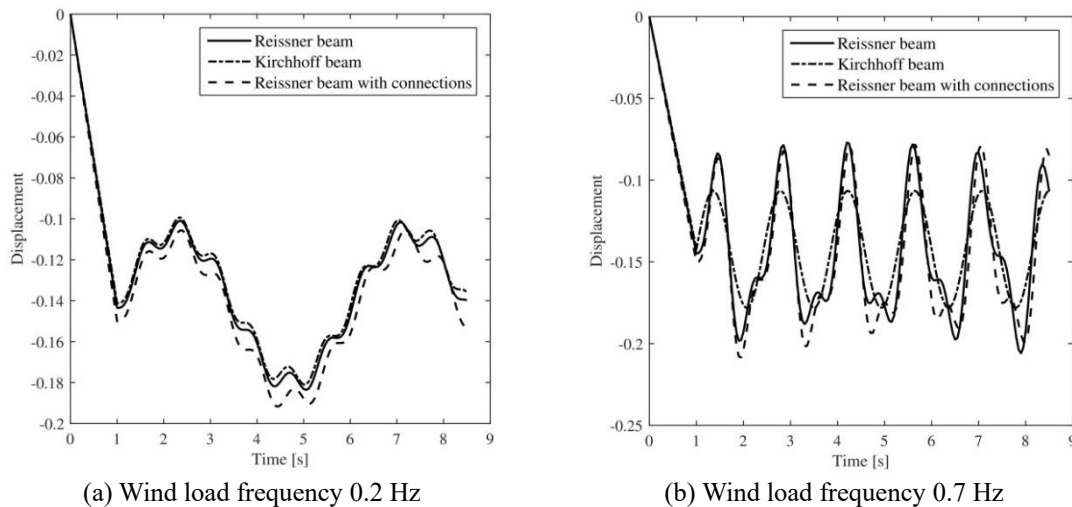


Fig. 9 Response of wind turbine structure-vibration amplitude

connections.

At the beginning of the computation, we performed the dynamic analysis of the free vibration problem to obtain structure frequency, which is equal to $T= 0.8\text{s}$ ($f=1/0.8 \text{ s}=1.25 \text{ Hz}$). Further, to research dynamic response related to a load frequency, we have performed three computations for different load frequencies (0,2 Hz, 0,7 Hz and 1.2 Hz), where the last very close to structure frequency and resonance phenomena can be expected.

Fig. 9 shows the response of structure for load frequencies that are not close to structure frequency, the resonance is not expected, and small vibration amplitudes were obtained by using

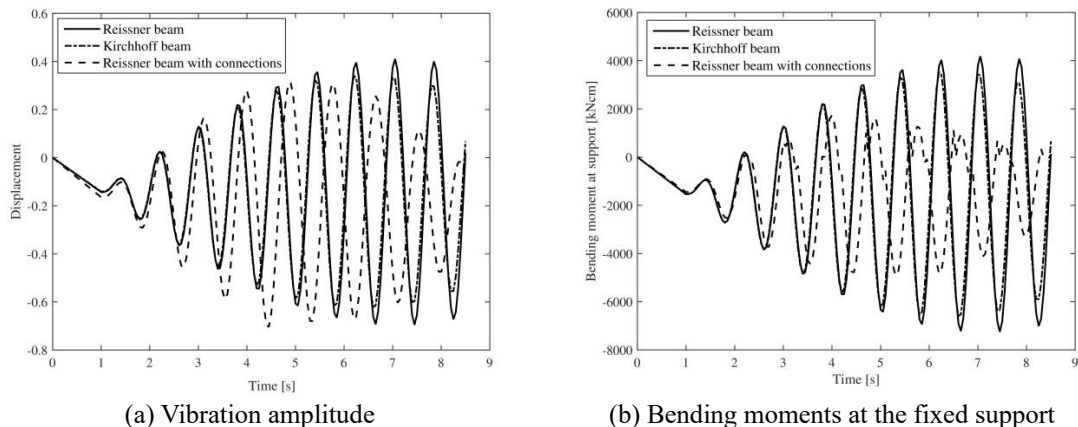


Fig. 10 Response of wind turbine structure under dynamic load with frequency 1.2 Hz

all calculation models. If we compare responses with and without connections we can see that effect of connection behavior in structure response is not significant, because plastic deformations have not occurred in connections.

In order to explore the effects of connection behavior on the dynamic response of the structure, we have performed the analysis with different beam models for a load frequency 1.2 Hz, which is close to the structure frequency 1.25 Hz. In Fig. 10, we can see that connections behavior increases vibration amplitude to the reaching yield bending moment, after that plastic hinges placed in connections change structure stiffness, dissipate energy, and damping vibrations amplitude. By analyzing the observed phenomena, we can conclude that connection behavior can be crucial in avoiding resonance by changing the stiffness of the structure and by damping vibration by developing plastic deformation.

3.3 Wind turbine installed between two parts of a building including temperature variation

The temperature variations can be large, which causes significant additional stress in steel elements if axial displacements at the ends are restrained. For example, in Sarajevo, Bosnia and Herzegovina, the average annual temperature is 10°C, while the maximal summer temperature is 40°C and the minimum winter temperature is -20°C, which is a temperature variation of $\Delta T = \pm 30^\circ\text{C}$.

In this example we analyze the steel structure shown in Fig. 8, but including temperature variations. The temperature is included by support displacements as load, which can be defined

$$\Delta L = \alpha_T \Delta T L \quad (25)$$

where α_T is thermal expansion coefficient.

To research the impact of temperature variations on the dynamic response of the structure, we have performed computation with different constitutive models for dynamic load with a frequency 1.2 Hz. For this case, structure and load frequency are close to what is leading to resonance. The linear-elastic response is shown in Fig. 11(a), where we can see increasing vibration amplitude leading to resonance. In shown results, maximal temperature causes compression force in structure

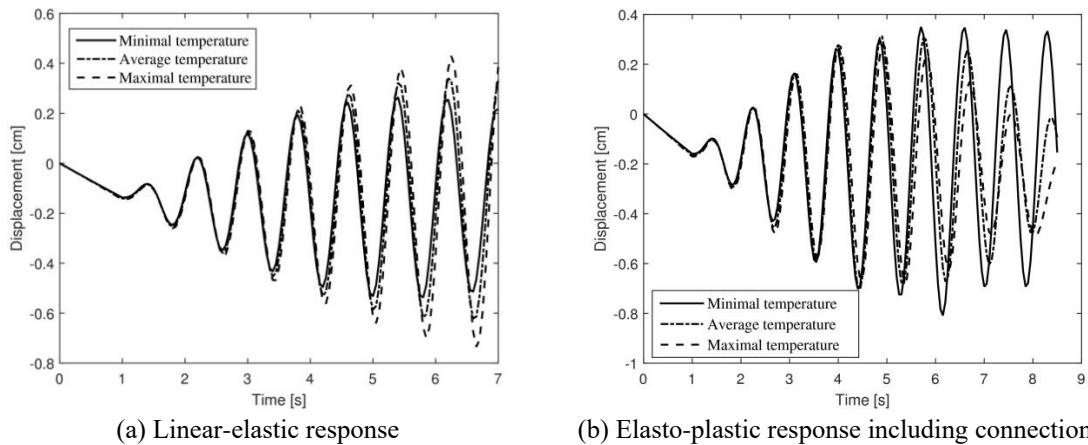


Fig. 11 Response of wind turbine structure under dynamic load with frequency 1.2 Hz

which makes the vibration problem worst.

On the other hand, the material does not behave linear-elastic for large stresses, because the linear-elastic calculation is not suitable. The elastoplastic response with included connection behavior is shown in Fig. 11(b), where we can see completely different results in comparison with Fig. 11(a). Namely, compression force caused by positive temperature increase vibration amplitude and stresses in structure activating plastic criterion earlier and damping vibration by dissipation energy to plastic deformations.

By analyzing the presented results can be stated, that temperature variation makes the vibration problems worst and has to be included in the design of the structure.

3.4 Innovative design of small wind turbine support steel structure

In this example, we propose an innovative design of the steel structure that includes cheap and simple frictional dampers. This type of structure can be installed on the new or existing buildings, while the frictional dampers can be set according to technical data of wind turbines.

The focus of the example is to reduce vibration amplitude during extreme wind conditions. The main idea is that we can localize deformations in previously designed joints and dissipate energy by friction in them, and after the end of extreme conditions easily return structure to the initial position.

The constitutive model for bending of innovative joints can be represented by the plastic model presented in Section 2, where those parameters have clear physical meaning and can be easily determined. Namely, the first, yielding bending moment $M_{j,y}$ corresponds to the bolt friction resistance which depends on applied pretension force, while joint hardening stiffness S_j is directly proportional to spring stiffness.

This type of innovative joint solution provides easily returning in the initial structure configuration by releasing bolts and pushing back, on the other side we can define the value of yielding bending moment and activation only for extreme wind conditions and different wind turbines.

The results of computation, shown in Fig. 13, present the effects of frictional dampers on dynamic response, which plays a crucial role in avoiding resonance. Linear-elastic response (Fig.

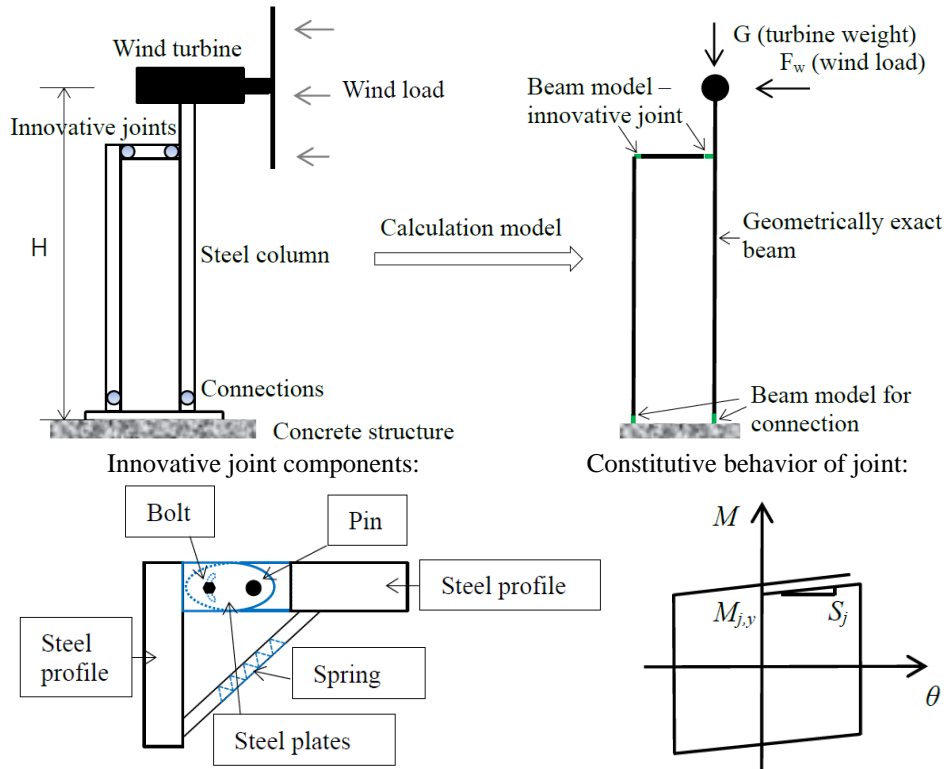


Fig. 12 Wind turbine structure with innovative joints

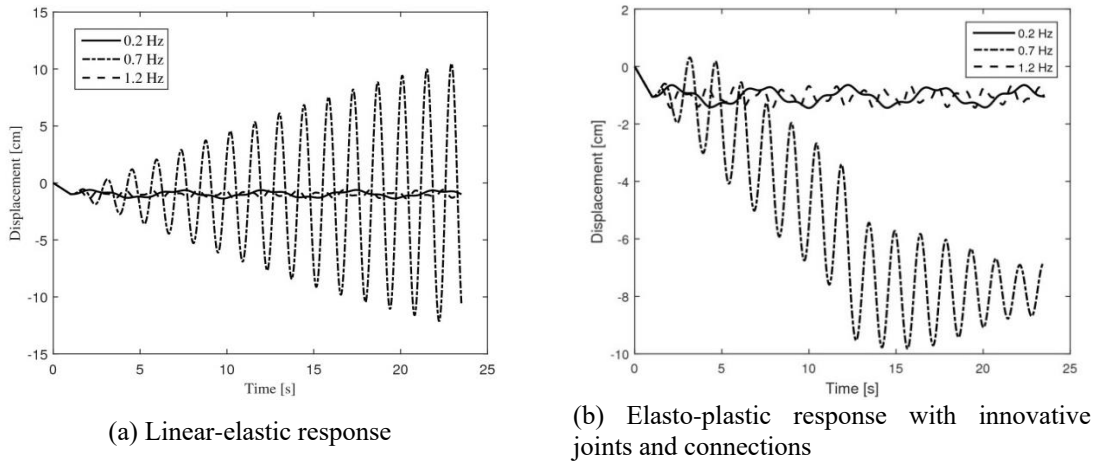


Fig. 13 Response of wind turbine structure with innovative joints

13(a)) indicates that resonance is happened for load frequency equal to 0.7 Hz, while the response with innovative joints (frictional dampers) avoids it. The programmed yielding in innovative joints causes additional inclination of the steel structure but decreases vibration amplitude and dynamic effects.

The bending moments in connections and steel elements are lower than the yielding values, so that structure is not damaged and can be used after extreme conditions with very easy reparation.

4. Conclusions

In this work we have presented an advanced approach to the design of small wind turbine support steel structures, by using improved versions of previously developed geometrically exact beam models. Namely, three different geometrically exact beam models are used, the first two are the Reissner and the Kirchhoff beam models implementing bi-linear hardening response and the third is the Reissner beam capable of also representing connections response. With these advanced models, we have performed analysis of four practical solutions for the installation of small wind turbines in new or existing buildings including the effects of elastoplastic response to vibration problems.

The numerical simulations confirm the robustness of numerical models in analyzing vibration problems and the ability to include the effect of elastoplastic response, which is crucial in avoiding resonance phenomena. In all examples, the plastic response reduces vibration amplitude, but it can cause additional inclination of the structure.

The last numerical simulation of a support structure with innovative joints, which have the function of frictional dampers, is the solution that we propose for the installation of small wind turbines on a new or existing building in an urban area.

The proposed advanced methodology is a powerful tool for the design of small wind turbine support structures and provides the capability in considering the ultimate loads and real structure elastoplastic response that is crucial for vibration issues.

Acknowledgments

The research described in this paper was financially supported by the Ministry of Education, Science and Youth of Sarajevo Canton, Bosnia and Herzegovina and MAEA funding for project CESP.A.

References

- Boujelben, A., Ibrahimbegovic, A. and Lefrançois, E. (2020), "An efficient computational model for fluid-structure interaction in application to large overall motion of wind turbine with flexible blades", *Appl. Math. Model.*, **77**, 392-407. <https://doi.org/10.1016/j.apm.2019.07.033>.
- Dujc, J., Bostjan, B. and Ibrahimbegovic, A. (2010), "Multi-scale computational model for failure analysis of metal frames that includes softening and local buckling", *Comput. Meth. Appl. Mech. Eng.*, **199**, 1371-1385. <https://doi.org/10.1016/j.cma.2009.09.003>.
- EN 1993-1-8 (2005), Eurocode 3: Design of Steel Structures-Part 1-8: Design of Joint, Bruxelles: European Committee.
- Faella, C., Piluso, V. and Rizzano, G. (2000), *Structural Steel Semirigid Connections: Theory, Design, and Software*, CRC Press LLC.
- Hajdo, E., Mejia-Nava, R.A., Imamovic, I. and Ibrahimbegovic, A. (2021), "Linearized instability analysis of frame structures under nonconservative loads: Static and dynamic approach", *Couple. Syst. Mech.*,

- 10**(1), 79-102. <https://doi.org/10.12989/csm.2021.10.1.079>.
- Hajdo, E., Ibrahimbegovic, A. and Dolarevic, S. (2020), "Buckling analysis of complex structures with refined model built of frame and shell finite elements", *Couple. Syst. Mech.*, **9**, 29-46. <https://doi.org/10.12989/csm.2020.9.1.029>.
- Hill, R. (1950), *The Mathematical Theory of Plasticity*, Clarendon Press, Oxford.
- Ibrahimbegovic, A. (1995), "On finite element implementation of geometrically nonlinear Reissner's beam theory: Three-dimensional curved beam elements", *Comput. Meth. Appl. Mech. Eng.*, **122**(1-2), 11-26. [https://doi.org/10.1016/0045-7825\(95\)00724-F](https://doi.org/10.1016/0045-7825(95)00724-F).
- Ibrahimbegovic, A. (2009), *Nonlinear Solid Mechanics*, Springer.
- Ibrahimbegovic, A. and Frey, F. (1993), "Finite element analysis of linear and non-linear planar deformations of elastic initially curved beam", *Int. J. Numer. Meth. Eng.*, **36**, 3239-3258. <https://doi.org/10.1002/nme.1620361903>.
- Ibrahimbegovic, A. and Mejia Nava, R.A. (2021), "Heterogeneities and material-scales providing physically-based damping to replace Rayleigh damping for any structure size", *Couple. Syst. Mech.*, **10**(3), 201. <https://doi.org/10.12989/csm.2021.10.3.201>.
- Imamovic, I., Ibrahimbegovic, A., Knopf-Lenoir, C. and Mesic, E. (2015), "Plasticity-damage model parameters identification for structural connections", *Couple. Syst. Mech.*, **4**, 337-364. <https://doi.org/10.12989/csm.2015.4.4.337>.
- Imamovic, I., Ibrahimbegovic, A. and Hajdo, E. (2019), "Geometrically exact initially curved Kirchhoff's planar elasto-plastic beam", *Couple. Syst. Mech.*, **8**(6), 537-553. <https://doi.org/10.12989/csm.2019.8.6.537>.
- Imamovic, I., Ibrahimbegovic, A. and Mesic, E. (2017), "Nonlinear kinematics Reissner's beam with combined hardening/softening elastoplasticity", *Comput. Struct.*, **189**, 12-25. <https://doi.org/10.1016/j.compstruc.2017.04.011>.
- Imamovic, I., Ibrahimbegovic, A. and Mesic, E. (2018), "Coupled testing-modeling approach to ultimate state computation of steel structure with connections for statics and dynamics", *Couple. Syst. Mech.*, **7**(5), 555-581. <https://doi.org/10.12989/csm.2018.7.5.555>.
- Reissner, E. (1972), "On one-dimensional finite-strain beam theory: The plane problem", *J. Appl. Math. Phys. (ZAMP)*, **23**, 795-804. <https://doi.org/10.1007/BF01602645>.